Cook, R., Wales, C. J. A., Gaitonde, A. L., Jones, D. P., & Cooper, J. E. (2017). Uncertainty Quantification in Gust Loads Analysis of a Highly Flexible Aircraft Wing. In *2017 International Forum on Aeroelasticity and Structural Dynamics (IFASD 2017): 25-28 June 2017, Como - Italy*
http://congressi.fondazionealessandrovolta.it/ifasd2017

Peer reviewed version

International Forum on Aeroelasticity and Structural Dynamics
IFASD 2017
25-28 June 2017 Como, Italy

UNCERTAINTY QUANTIFICATION IN GUST LOADS ANALYSIS OF A HIGHLY FLEXIBLE AIRCRAFT WING

Robert G. Cook[1], **Chris J. A. Wales**[1], **Ann L. Gaitonde**[1], **Dorian P. Jones**[1], **Jonathan E. Cooper**[1]

[1]Department of Aerospace Engineering, University of Bristol
Queen's Building, University Walk, Bristol, BS8 1TR, United Kingdom
Contact Author: robert.cook@bristol.ac.uk
Project Website: http://www.aerogust.eu

Keywords: structural dynamics, nonlinear aeroelasticity, geometric structural nonlinearity, uncertainty quantification, polynomial chaos expansion

Abstract: In this work, a typical industrial gust loads process has been adapted for use with a nonlinear aeroelastic system. This gust loads process is carried out to determine the worst case "1-minus-cosine" loads on different flexibility variations of a representative, high-aspect ratio, UAV wing, which is subject to uncertain atmospheric and structural properties. Polynomial chaos expansion-based techniques are then used to replicate the map from input uncertainty to the output uncertainties of particular quantities of interest. The results obtained from the nonlinear analysis are compared to linear results to understand what effect nonlinearities have on the propagation of uncertainties through the system. Significant differences in the linear and nonlinear outputs are found using deterministic analyses alone, but additionally, the uncertainty bounds also show differences. For example, for some quantities such as static loads or angle of attack the uncertainty bounds are higher for the nonlinear system than for the linear system. However, the opposite is seen for most of the gust loads, apart from root torque loads on the most flexible case, indicating that the effect of nonlinearities on uncertainty propagation can not be easily generalised. Furthermore, the necessity for round-the-clock gusts for highly flexible aircraft is highlighted.

1 INTRODUCTION

Recent developments of next-generation aircraft indicate that lighter, high-aspect ratio structures and higher flight speeds will become necessary in order to meet environmental targets of Flightpath 2050 and customer requirements of reduced flight times. As a result of exploring these new designs, it has become increasingly clear that nonlinear behaviour will become an important factor of the design process. Nonlinear behaviour may be associated with the structure (large structural deformations, complex planforms, large rigid body motions, etc.) or aerodynamic (transonic shock, local stall effects, etc.). There is currently much interest in the design of high-aspect ratio wing (HARW) aircraft which are strongly influenced by nonlinear geometric effects [1–3].

It is apparent that these nonlinear effects must be addressed from an industrial point of view to provide knowledge of their impact on aircraft behaviour by developing new tool-sets for loads prediction on the nonlinear system. These tools must also be computationally inexpensive, with comparable solution times to linear methods, in order to cope with the necessity of running large

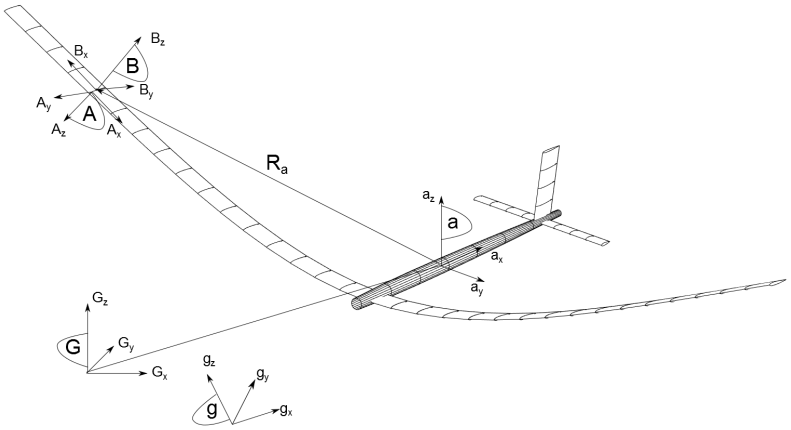

Figure 1: An illustration of a highly flexible aircraft in a trim flight shape.

numbers of simulations in a reasonable time frame. Furthermore, the methods explored should also reduce the reliance on costly wind tunnel testing for correcting the aeroelastic system by investigating CFD-based alternatives in order to include high-fidelity methods earlier in the design process.

One important issue with regards to aeroelastic design is understanding how the sensitivity of certain interesting quantities (IQs) change with system parameters. Knowledge of this uncertainty is a powerful tool to increase robustness of a gust loads process with respect to unknown or uncertain inputs to the equations of motion. Sensitivity analysis is also a key part of optimisation processes, and a good understanding of this would allow for more efficient gradient-based design procedures and more rapid design generation. An efficient uncertainty quantification (UQ) process will enable both robust and reliable designs to be made. There has been much work on UQ of aeroelastic structures [4, 5], particularly on gust loads analysis [6], but none so far on highly flexible aircraft. The focus on this particular work is not only to understand what difference nonlinearities have on the behaviour of flexible aircraft in addition to numerous other studies, but furthermore how the nonlinearities affect the propagation of uncertainties through the system.

2 METHODOLOGY

The approach used in this work will be described in this section. First, an overview of the nonlinear aeroelastic methodology will be presented, followed by a definition of the gust loads process that will be adapted from the industrial process for nonlinear systems. Finally, the uncertainty quantification techniques used are outlined.

2.1 Nonlinear Aeroelastic Modelling

A nonlinear aeroelastic approach is required to simulate highly flexible aircraft structures. The particular method used in this paper is described more in depth in Ref. [7], but will be outlined briefly here.

2.1.1 Nonlinear Structural Modelling

Nonlinearities that are considered in this work are in the form of geometrically-exact deformations. In order to capture such nonlinear structural behaviour, an intrinsic beam formulation, as

presented by Hodges [8], is used. In this approach, load-to-strain relationships are assumed to be linear, so no material nonlinearities are included. A piecewise-linear finite-element approach is used to solve the intrinsic beam equations, in a similar scheme to that used in Ref. [9], but rather than in a mixed-formulation, the intrinsic variables of local beam velocities, strains and curvatures are solved for directly; displacements and orientations are determined as temporal integration of the velocities or spatial integrals of the strains and curvatures.

2.1.2 Unsteady Aerodynamics

In this approach, the aerodynamics model used is a linear strip theory. Unsteady effects can be included into the formulation using Leishman's indicial response method [10] using Jones' approximation to Theodorsen's function [11]. Lift curve slopes are included from a standard vortex-lattice solver to include three-dimensional lift distributions that are not automatically determined in a strip theory formulation.

2.1.3 Numerical Implementation

The coupled nonlinear structural and unsteady aerodynamics formulation is coded in MATLAB. The static equations are solved using a Newton-Raphson iterative approach, and the dynamic equations are solved using a Newmark-β-type solver, in a scheme based on Ref. [12]. Trim conditions are achieved by applying an additional, outer Newton-Raphson loop to the static solution to balance forces.

2.2 A Gust Loads Process for Nonlinear Systems

In this work, discrete, 1-minus-cosine (1MC) gusts will be considered as disturbances on the system; the number of gust lengths considered, $N_H \in \mathbb{N}$, is defined in EASA [13] and FAA [14] guidelines to be 'a sufficient number', between the regulation maximum and minimum lengths; this work will consider 11 equally spaced gust lengths from 20m to 220m.

A typical gust loads process used in industry [15] assumes linearity, which is valid for small deformations and rigid body rotations, and which greatly simplifies the procedure. Under linear assumptions, trim/static loads analyses can be carried out independently of gust loads analyses (the gust loads are usually obtained from the undeformed geometry), and total loads are obtained simply by adding together the static and enveloped gust loads as a post-process. Furthermore, only vertical and lateral gusts need be considered, as negative gusts and round-the-clock (RTC) gusts can also be calculated in a post-process from the original gust loads analyses. Therefore, for a linear system for a given flight and mass case, only one trim solution is required, and N_H vertical and N_H lateral gust simulations are required ($2N_H$ gust simulations in total).

Once aeroelastic nonlinearities are considered, the gust loads process must be adapted. Gust loads analyses are carried out about the trim geometry, rather than the undeformed geometry, in order to account for geometric and aerodynamic damping effects. Furthermore, it can be assumed that due to large deformations, the worst case gust may not be due to purely vertical or lateral gusts, so additional gust directions must also be considered due to the fact that RTC gust loads can not be calculated directly for a nonlinear system. This effect means that for every gust length considered, a number of gust directions, $N_\theta \in \mathbb{N}$, should be run to capture the effects of angled gusts. Therefore, for a nonlinear system for a given flight and mass case, only one trim solution is still required, but now $N_H \times N_\theta$ gust simulations are required in total. In this work,

12 equally spaced gust orientations are considered from 0° to 330° in 30° increments. This is a relatively brute force approach by running a series of gust lengths and directions; more efficient approaches could potentially reduce this computational effort [16]. Future developments of this gust loads process could consider using gust angles determined from a RTC analysis on the system linearised about the trim condition to reduce N_θ by focusing the search on a more specific gust direction and decrease the number of computations required.

Static results are obtained from the full nonlinear code, and compared to results obtained from MSC.NASTRAN's static solution using doublet-lattice aerodynamics and a linear structural model. Gust loads are obtained from the full nonlinear code, as well as the same code linearised about the undeformed geometry (replicating the 'traditional' approach) and linearised about the trim geometry. This comparison is performed to understand the limits of the linear approach used widely in industry, but also to determine whether these differences are fundamentally due to linear assumptions explicitly, or the particular industrial implementation of the linear system about an undeformed shape.

2.3 Uncertainty Quantification

The uncertainty quantification approach will now be outlined. The aim of this work is to understand how uncertainties propagate through both linear and nonlinear gust loads processes, and what differences can be observed. The entire gust loads process can be simplified to a black-box-type relationship,

$$\mathbf{Y} = f(\mathbf{X}) \tag{1}$$

where $\mathbf{X} \in \mathbb{R}^{N_I}$ are variables which describe N_I inputs to the gust loads process and $\mathbf{Y} \in \mathbb{R}^{N_O}$ are N_O variables that are output from the gust loads process (maximum loads, worst case gust lengths, etc.). The function, f, is some mapping from $\mathbf{X}$ to $\mathbf{Y}$ which describes the gust loads process, and which is hard to describe algebraically for a complex system as used in this work, but nonetheless is easy to carry out for given values of $\mathbf{X}$. The mapping, f, could represent the linear or the nonlinear gust loads process, noting that for the linear gust loads process the dynamic aeroelastic system is linear, but not necessarily the mapping from input variable to output variable. The premise of UQ analysis is that certain system inputs, X_i, may not be known exactly, but may be known with some statistical distribution. Predicting how uncertainty on values of $\mathbf{X}$ propagates through the mapping, f, is the aim of these UQ techniques.

Next, the type, and nature of the uncertainties that enter the gust loads analysis are defined, followed by a description of the methods used to create reduced-order models (ROMs) of the I/O mapping in Eq. 1.

2.3.1 Uncertain Variables

In order to analyse the effect that uncertain input variables have on the system, first the uncertainties must be defined, both in terms of the exact sources of uncertainty, as well as the probability density functions (PDFs) that define them. Sources of uncertainty could be due to the environment (air temperature, air density, etc.); or could be found in the aircraft properties themselves (stiffness properties, mass properties, structural damping, etc.). Determining which

variables to consider as uncertain is relatively straightforward, but it is less clear from the literature and industry what kind of distributions the uncertainties will take. Furthermore, the greater the number of uncertain variables considered in a UQ analysis, the more computationally expensive the analysis becomes. Therefore, keeping the number of uncertainties for the study low and general can give a good insight into the behaviour without incurring excessive computation.

In this work, both environmental and aircraft property uncertainties will be considered. Specifically, it will be assumed that the air density, ρ_∞, Young's modulus, E, and shear modulus, G, are assumed to vary in a statistical manner about a baseline value. The baseline values are defined for a particular aircraft and flight case, which in turn define the mean values of the probability density functions that are used. A normal distribution is assumed (often the case with natural processes), and the standard deviation, σ is defined to be $3.\bar{3}\%$ of the mean value of that particular variable (i.e. approximately 99.7% of the possible values the variable can take fall within $\pm 10\%$ of the mean value).

The industrial gust loads process itself is considered to be deterministic, as defined by EASA [13] or FAA [14] airworthiness regulations on gusts.

2.3.2 Uncertainty Quantification Methods

Monte Carlo simulations (MCS) are a common method for approximating the outputs of the mapping in Eq. 1, and are popular for the relative ease of set-up, at the expense of running large numbers of simulations. However, in this particular study, an MCS is simply not feasible due to the sheer number of computations that would be required. Using the gust loads process defined in §2.2 for a full nonlinear aeroelastic system, with $N_u \in \mathbb{N}$ uncertain variables and $N_{X_i} \in \mathbb{N}$ number of gust loads processes required for a given uncertain variable, i, the required number of static simulations, $N_{sim_{stat}} \in \mathbb{N}$ is

$$N_{sim_{stat}} = \prod_{i=1}^{N_u} N_{X_i}, \tag{2}$$

and the required number of dynamic gust simulations, $N_{sim_{dyn}} \in \mathbb{N}$ is

$$N_{sim_{dyn}} = N_\theta N_H \prod_{i=1}^{N_u} N_{X_i}. \tag{3}$$

Typically in an MCS, the number of samples for all uncertain variables, N_{X_i}, should be as large as possible, and so for even low numbers of uncertain parameters, N_u, the number of simulations can quickly become impractical (1,000 simulations, say, for combinations of all 3 uncertain variables, i.e., $N_{X_1} = N_{X_2} = N_{X_3} = 1000$, considered in this paper results in $1{\times}10^9$ trim cases and $132{\times}10^9$ gust simulations). While a Latin hypercube sampling (LHS) can reduce the total number of simulations required, even if $\prod_{i=1}^{N_u} N_{X_i}$ could be sampled to 1,000 combinations in total, that still represents a huge number of simulations. Therefore it can be seen that the number of simulations run, N_{X_i}, must be reduced in order to study the effects of multiple uncertain variables without excessive computational effort. This is achieved using polynomial chaos expansion (PCE) [17] techniques to create ROMs of the mapping between uncertain variables and interesting quantities (IQs). In this approach, the gust loads mapping,

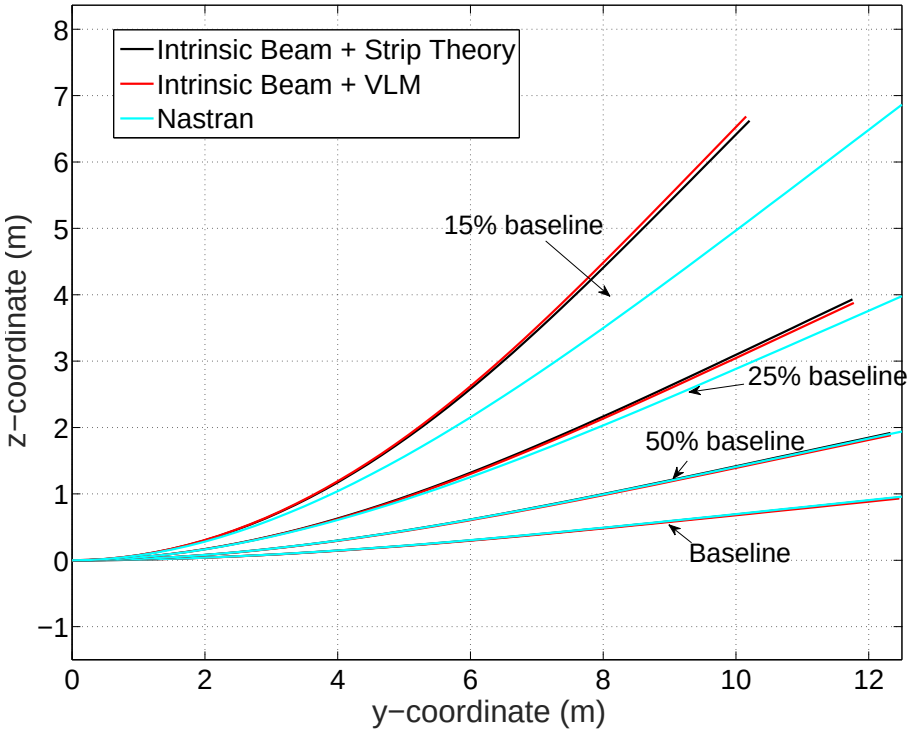

Figure 2: Trim shapes of the flexible variants of the UAV wing used in this work.

f, in Eq. 1 is approximated using polynomials of a particular type depending on the input uncertainty PDFs (Hermite polynomials are used for normal distributions). The coefficients of these polynomials are determined through a least-squares fitting process based on the inputs and outputs of a set of deterministic simulations on the mapping, f. Computing the mapping this way requires a smaller number of sample points, N_{X_i} as compared to a MCS for example.

In this work, with $N_u = 3$, and $N_{X_i} = 5$, the total number of trim cases is 125, and the number of gust simulations required is 16,500. This is a significant reduction compared to a Monte Carlo simulation, but still represents a considerable computational effort. Future work will consider reducing this number further still by producing surrogate models of the gust loads process, which could reduce N_H and N_θ, in addition to using more novel UQ methodologies that can predict uncertainties with even fewer simulations required that PCE methods.

3 TEST CASE DEFINITION

The specific test case that is being studied in this work is a representative high aspect ratio (HAR) UAV wing, designed for the AEROGUST project [18]. The wing is based roughly on the size and modal response of a Global Hawk, and has an aspect-ratio of 25 and uniform chord of 2m. It is unswept, untapered, with no dihedral or twist, and fixed at the root with a cantilever boundary condition. The individual wing mass is 425kg and the full aircraft mass is 7,000kg. The structure of the wing is defined as a simple rectangular section with constant outer dimensions (a width of 1m and height of 0.2m), and a linearly varying thickness (from 6mm at the root to 1.5mm at the tip). The centre of this rectangular section lies 40% chord behind the leading edge, and is made of aluminium with Young's modulus of 69GPa, and a shear modulus of 27GPa. The first, second and third bending modes occur at 1.79Hz, 9.84Hz, and 26.35Hz, respectively; the first torsion mode occurs at 15.26Hz; and the first fore-aft/in-plane bending

mode occurs at 25.23Hz. The flight case for this aircraft is an altitude of 55,000ft at Mach 0.5, although the compressibility effects are ignored in the aerodynamics models used.

Despite the baseline wing having quite a high aspect ratio, it is still fairly stiff, and therefore under normal flight conditions does not exhibit large deformations. To encourage larger deformations and emphasise the effects of geometric nonlinearity on the behaviour of the wing, flexible variants of the wing are created by multiplying the stiffness properties of structure by some factor. Figure 2 shows the trim geometry of the wing as seen from the front, comparing the intrinsic beam approach with both vortex lattice method (VLM) and modified strip theory aerodynamics, to a linear approach using MSC.NASTRAN (linear structure and doublet-lattice aerodynamics). It can be seen how the baseline and 50% stiffness wing trim shape agrees very well with the results of MSC.NASTRAN, but at 25% of the baseline stiffness and below, tip shortening effects can be seen in the nonlinear code that are not present in the linear analysis. Additionally, it can be seen that there is little difference, even at high deformations, between modified strip theory and VLM, even though the strip theory is given a lift distribution based on the undeformed geometry. Below 15% of the baseline stiffness, the wing is unable to generate sufficient lift to be able to be trimmed.

The structural properties and air density defined here form the mean values used in the UQ analysis, with the standard deviations defined as in §2.3.1.

4 RESULTS

The results of the UQ analysis on the aforementioned HAR UAV test case will be presented here. First, the UQ analysis on the static loads are shown, followed by the UQ analysis on the gust loads.

4.1 Static UQ Analysis

For the static results, the wing is trimmed to balance the total gravitational forces including a lumped mass at the root representative of fuselage and payload mass. The analysis is carried out deterministically at first as a reference, using the mean values of air density and structural properties. This process is then repeated for the 125 combinations of air density, Young's modulus and shear modulus.

Figure 3 shows how the trim angle of attack varies as the baseline wing is made more flexible, comparing MSC.NASTRAN to the nonlinear method used in this work. It can be seen that there is good agreement for the baseline wing, but there is a completely opposite trend as the wing is made more flexible. In the nonlinear analysis, the effect of large deformations causes a component of the normal aerodynamic force to act inboard, reducing the lift and requiring a larger angle of attack to compensate; the linear analysis always assumes normal force to act vertically. It can be seen from the polynomial chaos analysis that the mean value obtained from the probabilistic output matches the deterministic values very well (which is not necessarily guaranteed, see for example Ref. [19]). In addition to the mean values, error bars are included that represent an interval such that approximately 99.7% of the outputs fall subject to the uncertain inputs. Here it can be seen that the uncertainties of the output are similar between the linear and the nonlinear at the baseline stiffness, but the bars increase in length for the nonlinear system as it becomes more flexible. In contrast, the error bars remain fairly constant in length for all flexibilities in the linear system. Not included here for brevity are plots of higher-order

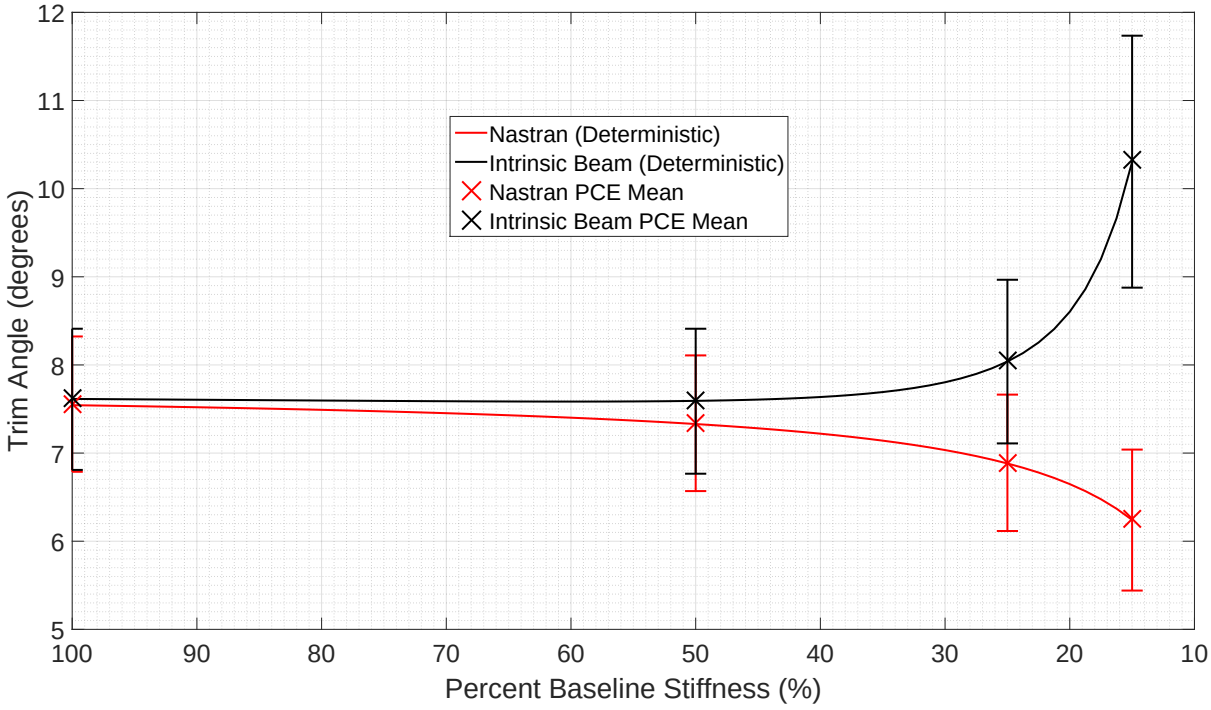

Figure 3: Angle of Attack vs. Percent Baseline Stiffness, comparing deterministic results to the mean values obtained from PC analysis. Error bars represent the bounds within which ≈99.7% of the outputs fall subject to variable inputs.

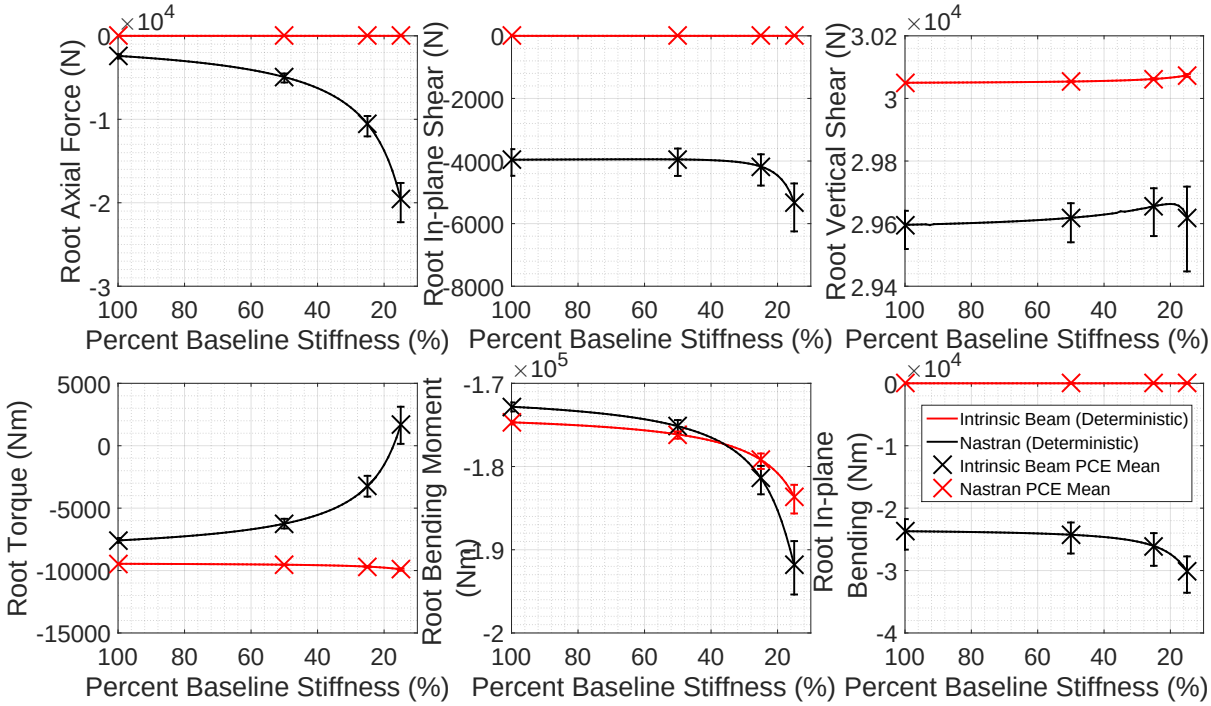

Figure 4: Root Loads vs. Percent Baseline Stiffness, comparing deterministic results to the mean values obtained from PC analysis. Error bars represent the bounds within which ≈99.7% of the outputs fall subject to variable inputs.

statistical moments. However, skewness and excess kurtosis were calculated and found to be fairly low indicating the output probability density functions are close to a normal distribution, with some skewness which can be seen in asymmetry of the error bars of Fig. 3.

In addition to angle of attack plots, the effect of uncertain variables can also be considered on the structural loads. Plotted in Fig. 4 are the trim loads, comparing deterministic loads using linear and nonlinear analyses, with the mean values from a UQ analysis. From the deterministic analysis, it can be seen how the root vertical shear remains fairly constant for both linear and nonlinear analyses, as would be expected due to the trim condition requiring a force balance. The behaviour of the root bending moment also matches well between the linear and the nonlinear. The biggest differences can be see in root axial force root in-plane shear force and root in-plane bending moment where the linear analysis predicts no loads at all, but the nonlinear predicts significant loading. Furthermore, the root torque is significantly different between the linear and nonlinear, and even displays a change of sign as the wing gets more flexible. This is due to components of lift in the nonlinear system that appear locally as in-plane forces, which in turn develop a counter-torque when the wing deforms, i.e. a vertical moment arm is formed. The linear analysis does not take this effect into account. From the PCE UQ analysis, the mean values match well with the deterministic values in a similar way as seen previously for the angle of attack plots. There are significant differences observed in the output uncertainty between the linear and nonlinear analyses; the linear analyses generally display very little uncertainty due to the input uncertainties, with exception of the root bending moment of the more flexible cases considered. In contrast, the nonlinear system appears to have a considerable sensitivity to the input uncertainties, which is probably more significant in the root torque loads. Again, higher-order statistical moments are not plotted here, but the output PDFs are largely normally distributed with a little skewness.

4.2 Gust Response UQ Analysis

With the trim calculations presented and analysed, the gust loads analyses on the linear (about undeformed and deformed geometries) and nonlinear systems can be presented. The gust loads are calculated as described in §2.2, for 125 combinations of air density, Young's modulus and shear modulus. The nonlinear and linear systems about the trim geometry are initialised from their respective trim condition determined earlier. The UQ of the structural loads will first be presented, and then a discussion about other output variables that can be analyses as part of the UQ work.

4.2.1 Gust Loads

The effect of uncertainties on the root gust loads can be seen in Figure 5, showing how the mean values of the gust loads PDFs vary with flexibility. It can be seen how, for root vertical shear force and root bending moment, the linearised system about the undeformed geometry over-predicts the loads, even for the stiffest case considered. The torque is greatly over-predicted by the linear system for stiffer wings, but as the wing becomes more flexible, the nonlinear system over-predicts. Axial force, in-plane shear force and in-plane bending are very small in the linear analysis, but exhibit contributions which are not insignificant in the nonlinear system. As perhaps expected, the system linearised about the trim geometry rather than undeformed geometry, give a much better match to the nonlinear system until the most flexible variant is considered.

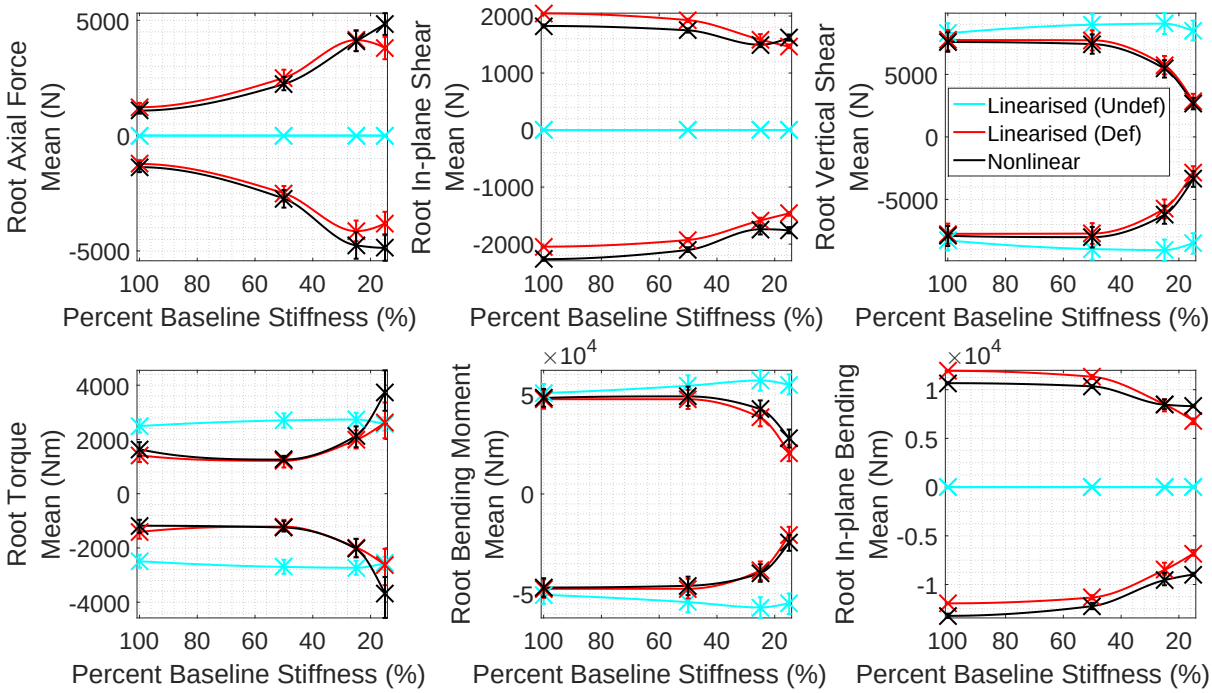

Figure 5: Worst case gust loads (incremental) vs. Percent Baseline Stiffness, comparing deterministic results to the mean values obtained from PC analysis. Error bars represent the bounds within which ≈99.7% of the outputs fall subject to variable inputs.

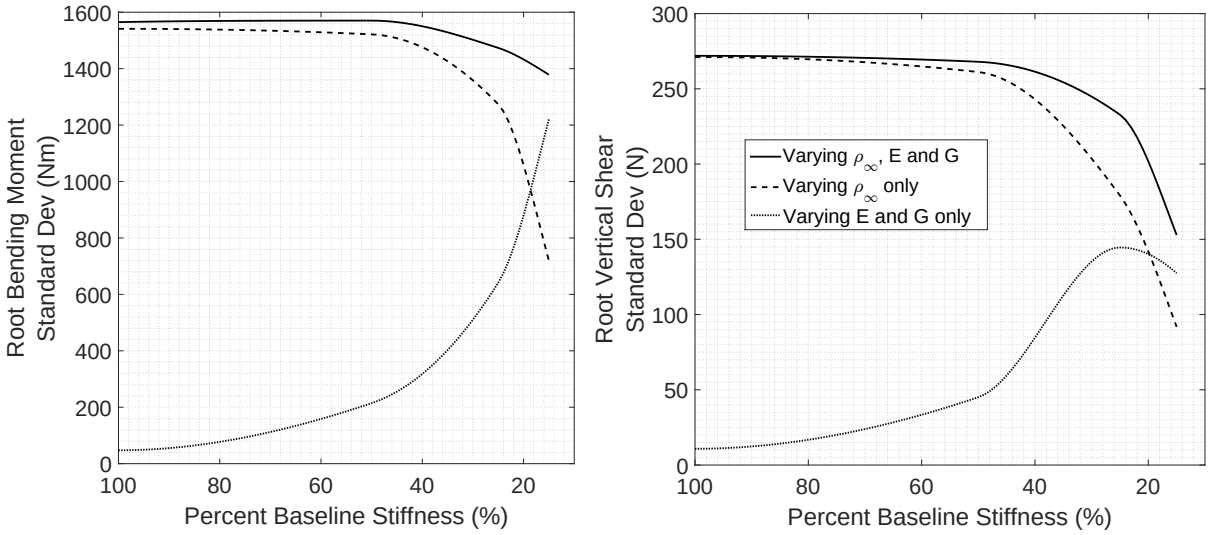

Figure 6: Comparison of the Standard Deviation vs. Percentage Baseline Stiffness on the nonlinear system.

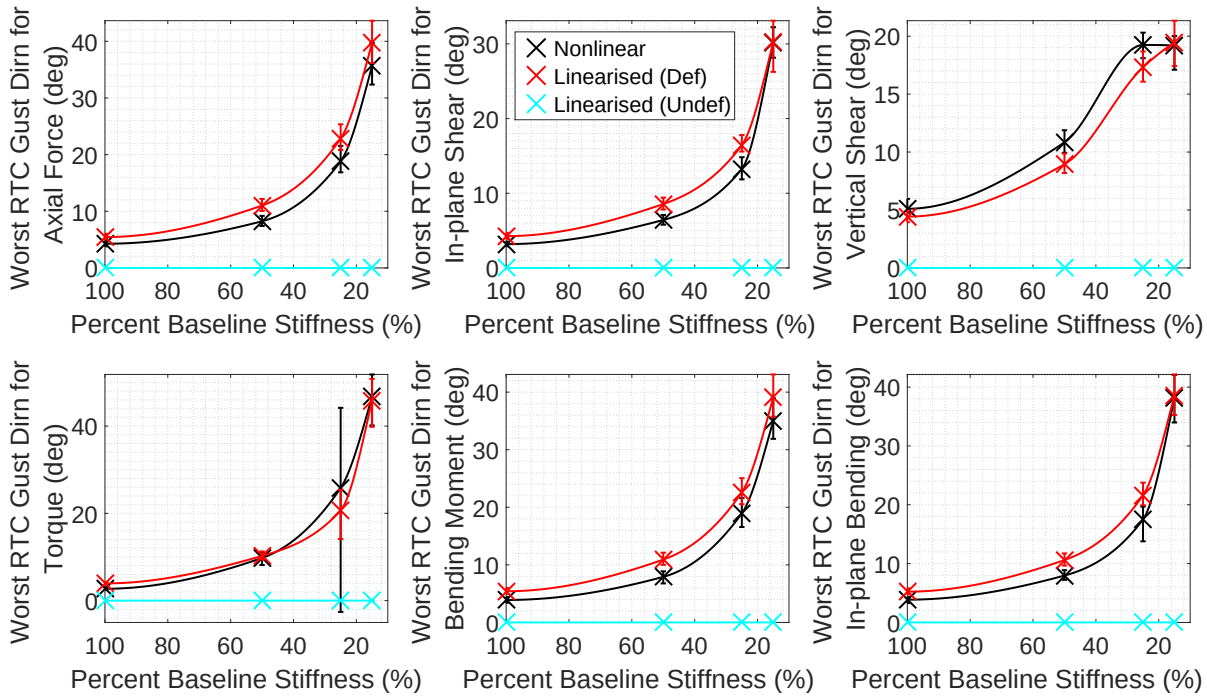

Figure 7: Worst case gust direction (RTC gust) vs. Percent Baseline Stiffness, comparing deterministic results to the mean values obtained from PC analysis. Error bars represent the bounds within which ≈99.7% of the outputs fall subject to variable inputs.

From the error bars representing the spread of the uncertainties in Figure 5, it can be seen for root vertical shear and bending that the uncertainty in the nonlinear system outputs decreases compared to the linear analysis, showing an opposite trend to results seen in the static loads and angle of attack. The same phenomena can be seen for the nonlinear analysis for the root torque until the most flexible case considered, where the uncertainties on the nonlinear system increase rapidly compared to linear analyses.

The uncertainty analysis is carried out once more on the gust loads of the nonlinear system only, considering cases where either the structural properties are kept fixed and the air density varies, or vice versa, with the standard deviations illustrated in Figure 6. It can be seen how air density uncertainties dominate root vertical shear and root bending moment uncertainties for the baseline case, but as it becomes more flexible, the standard deviation due to air density variations reduces. Conversely, structural property uncertainties have little impact on the loads uncertainties for the baseline, but they become more influential on the aircraft as it gets more flexible.

4.2.2 Worst Case Gust

It is also of interest to determine which gust length and direction has caused the worst case loads, and how flexibility and uncertainties affect this worst case. The worst case gust angle can be easily determined as the RTC gust angle in the linear analysis. The worst case gust angle for the nonlinear case, as well as the worst case gust length for the linear and nonlinear cases are not known exactly, but can be estimated using a cubic spline from the cases that have been run to interpolate between the known values.

Figure 7 shows how the worst case gust angle for different root loads changes with flexibility. It

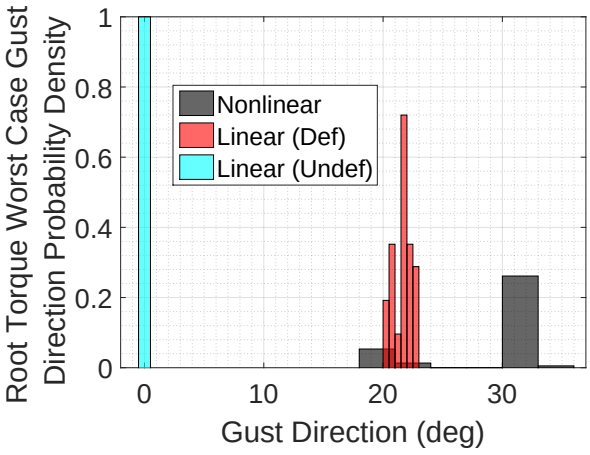

Figure 8: Maximum root torque histograms (normalised as a PDF).

can be seen from the RTC analysis on the linear system about the undeformed geometry that the worst case for all loads occurs due to a purely vertical force (RTC gust direction is near zero). The linear system about the trim geometry, however, suggests that even for the stiffest wing considered, a gust orientated around 5° from vertical would give consistently worst loads than a purely vertical or lateral gust. This angle increases as the aircraft gets more flexible, until for the 15% baseline case, gusts oriented between 20% to almost 45% would give the worst case loadings. This angle can be compared to the rough orientation of the midwing trim geometry in Figure 2. This result agrees well with those obtained from the nonlinear analysis, although it is hard to say which is more accurate; the RTC angles from the linear results have been calculated exactly from an approximation to the nonlinear system, while the RTC angles from the nonlinear system have been approximated from a spline from known values. The most obvious outlier in Fig. 7 is the nonlinear root torque uncertainty for the 25% baseline stiffness case, which exhibits a much larger spread of uncertainty than any other result. In this case, the worst case gust angle for the nonlinear system seems to fall between two distinct values, whereas in the linear analyses the data is more clustered about a single value. Figure 8 plots a histogram of the 125 simulations for linear undeformed, linear deformed and nonlinear and shows that the data splits quite clearly between two distinct values for the nonlinear analysis. This highlights interesting phenomena that can occur in the gust loads post-processes of determining the maximum and minimum envelopes, where the case defining worst loads can switch between to distinct gust inputs.

The worst case gust length for maximum root torque is plotted in Fig. 9, illustrating how as the wing becomes more flexible, the linear analysis about the undeformed geometry predicts the worst case gust length to increase. In contrast, the linear analysis about the trim geometry, and the nonlinear analysis, predict entirely opposite trends showing that the worst case gust length reduces with flexibility. In all analyses, it is clear that the maximum and minimum gust lengths defined in the regulations may not be sufficient as the aircraft becomes more flexible, and it may be necessary to extend the limits for this particular case. As it is not known for sure a priori that the worst case gust will exceed the regulation guidelines, and it has been demonstrated how increasing the number of gust cases to run can be expensive, this emphasises the need for surrogate models that can quickly scan the problem space to detect such features. In this way, additional, exceptional gust cases that may affect the results can be easily included into the analysis, minimising any extrapolation outside of the search space.

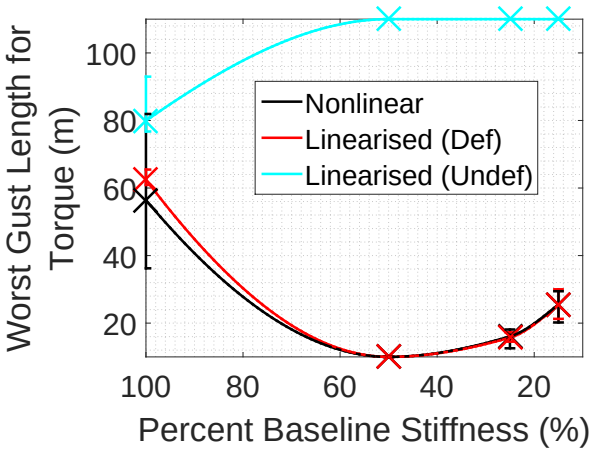

Figure 9: Worst case gust length vs. Percent Baseline Stiffness, comparing deterministic results to the mean values obtained from PC analysis. Error bars represent the bounds within which ≈99.7% of the outputs fall subject to variable inputs.

5 CONCLUSIONS

Polynomial chaos expansion techniques have been used to compare how uncertain outputs from linear and nonlinear gust loads differ, subject to uncertainty inputs.

From the static analyses, considerable differences can be seen between the linear and nonlinear trim results. The deterministic results how the angle of attack predictions showed opposite trends between the linear and nonlinear systems due to differences in how the aerodynamic forces are orientated. The mean values of the probability density functions obtained from polynomial chaos expansion computations match the deterministic analysis well, but from quantiles representing the uncertainty of the output, the uncertainties of the angle of attack increases with flexibility for the nonlinear case but remain fairly constant for the linear approach. Similar results occur in the loads, where uncertainties in the linear analysis generally remain low and constant as the wing becomes more flexible, but these uncertainties grew in the nonlinear system, particularly in torque.

In the gust loads analyses, the linear system about the undeformed geometry over-predicts root vertical shear and bending moment, as well as torque for the stiffer wings, when compared to the nonlinear system. However, for the most flexible case, the linear system under-predicts root torque. Unsurprisingly, the linear system about the trim condition gives much better results. Unlike with the static results, the uncertainties predicted by the nonlinear system generally reduced as the wing got more flexible, compared to results from the linear analyses which, again, remained fairly constant. Root torque on the most flexible case remains the exception to this generalisation, where the uncertainty increases drastically compared to linear results. For the stiffer wings it was demonstrated that the aerodynamic uncertainties were far more influential on the loads uncertainties compared to structural uncertainties, but the opposite was true for the most flexible wing considered. In addition to loads, the worst case gust cases were analysed, showing how the worst case gust orientation increases with flexibility, and highlights the necessity for round-the-clock calculations in gust loads calculations of very flexible aircraft.

Overall, the effects of nonlinearities can be seen to have a large impact on the aeroelastic behaviour compared to a linear analysis, even when only considering the deterministic results.

Inclusion of uncertainty analyses on the results highlights how nonlinearities also change the sensitivity of the system to certain variables, and it it not possible to generalise whether uncertainties in quantities of interest will increase or decrease relative to those calculated from equivalent linear analyses. However, it was clear that even for highly flexible variants of the wing considered here, linearising the system about the trim geometry seems to give a very good, and relatively computationally efficient, starting point to explore the problem space. Future work considering surrogate models, and uses of linear models about trim conditions, could reduce the number of computations carried out in this work to rapidly generate uncertainty results. This is particularly relevant considering results seen here looking at the worst case gust length, where the regulation gusts were not sufficiently long or short to capture certain worst case gusts. It would therefore be necessary to be able to determine these cases quickly and efficiently.

ACKNOWLEDGEMENTS

The research leading to these results has received funding from the AEROGUST project (funded by the European Commission under grant agreement number 636053). The partners in AEROGUST are: University of Bristol, INRIA, NLR, DLR, University of Cape Town, NUMECA, Optimad Engineering S.r.l., University of Liverpool, Airbus Defence and Space, Dassault Aviation, Piaggio Aerospace and Valeol.

6 REFERENCES

[1] Howcroft, H., Cook, R. G., Calderon, D. E., et al. (2016). Aeroelastic Modelling of Highly Flexible Wings. In *57th AIAA/ASCE/AHS/ASC Structures, Structural Dynamics, and Materials Conference*. San Diego, California.

[2] Bradley, M. K. and Droney, C. K. (2011). Subsonic ultra green aircraft research. *NASA/CR-2011-216847*.

[3] Allen, T. J., Sexton, B. W., and Scott, M. J. (2015). SUGAR Truss Braced Wing Full Scale Aeroelastic Analysis and Dynamically Scaled Wind Tunnel Model Development. In *56th AIAA/ASCE/AHS/ASC Structures, Structural Dynamics, and Materials Conference*. Kissimmee, Florida.

[4] Tartaruga, I., Cooper, J. E., Sartor, P., et al. (2016). Geometrical based method for the uncertainty quantification of correlated aircraft loads. *Journal of Aeroelasticity and Structural Dynamics*, 4(1), 1–20.

[5] Manan, A. and Cooper, J. E. (2009). Design of composite wings including uncertainties: A probabilistic approach. *Journal of Aircraft*, 46(2), 601–607.

[6] Khodaparast, H., Georgiou, G., Cooper, J. E., et al. (2011). Efficient Worst Case "1-cosine" Gust Loads Prediction. In *15th International Forum on Aeroelasticity and Structural Dynamics*, IFASD-2011-048. Paris, France.

[7] Cook, R., Calderon, D., Coetzee, E., et al. (2017). Worst Case Gust Prediction of Highly Flexible Wings. In *58th AIAA/ASME/ASCE/AHS/ASC structures, structural dynamics, and materials conference*, AIAA Paper No. 2017-1355. Grapevine, Texas. doi:10.2514/6.2017-1355.

[8] Hodges, D. H. (1990). A mixed variational formulation based on exact intrinsic equations or dynamics of moving beams. *International Journal of Solids and Structures*, 26(11), 1253–1273.

[9] Hodges, D. H., Shang, X., and Cesnik, C. E. S. (1996). Finite element solution of nonlinear intrinsic equations for curved composite beams. *Journal of the American Helicopter Society*, 41(9).

[10] Leishman, J. G. (1994). Unsteady lift of a flapped airfoil by indicial concepts. *Journal of Aircraft*, 31(2), 288–297.

[11] Jones, W. P. Aerodynamic forces on wings in nonuniform motion. *ARCR & M 2117*.

[12] Shearer, C. M. and Cesnik, C. E. S. (2006). Modified Generalized-α Method for Integrating Governing Equations of Very Flexible Aircraft. In *47th AIAA/ASME/ASCE/AHS/ASC Structures, Structural Dynamics, and Materials Conference*, AIAA 2006-1747. Newport, Rhode Island.

[13] European Aviation Safety Agency (EASA) (2003). *CS-25 Certification Specifications for Large Aeroplanes*.

[14] FAA Federal Aviation Regulations, Section 25.341. `http://www.flightsimaviation.com/data/FARS/part_25-341.html`. Accessed: 2017-06-01.

[15] Wright, J. R. and Cooper, J. E. *Introduction to Aircraft Aeroelasticity and Loads*. Wiley.

[16] Khodaparast, H. H., Cooper, J. E., Cavagna, L., et al. (2013). Fast prediction of worst case gust loads. In *International Forum on Aeroelasticity and Structural Dynamics, 2013*. Bristol, UK.

[17] Ghanem, R. G. and Spanos, P. D. (2003). *Stochastic Finite Elements: A Spectral Approach*. Courier Corporation.

[18] AEROGUST project (funded by the European Commission under grant agreement number 636053). `https://www.aerogust.eu`. Accessed: 2017-05-26.

[19] Wunsch, D., Nigro, R., Coussement, G., et al. (2015). Uncertainty Quantification of Simultaneous Operational and Geometrical Uncertainties in Turbomachinery Design Practice. In *International Gas Turbine Congress 2015 Tokyo*. Tokyo, Japan.

COPYRIGHT STATEMENT